International Journal of Bifurcation and Chaos, Vol. 17, No. 1 (2007) 183–198

LOCAL AND GLOBAL BIFURCATIONS TO LIMIT CYCLES IN A CLASS OF LIÉNARD EQUATION

PEI YU
Department of Applied Mathematics, The University of Western Ontario,
London, Ontario N6A 5B7, Canada
pyu@pyu1.apmaths.uwo.ca

Received June 14, 2005; Revised January 23, 2006

In this paper, we study limit cycles in the Liénard equation: $\ddot{x} + f(x)\dot{x} + g(x) = 0$ where $f(x)$ is an even polynomial function with degree $2m$, while $g(x)$ is a third-degree, odd polynomial function. In phase space, the system has three fixed points, one saddle point at the origin and two linear centers which are symmetric about the origin. It is shown that the system can have $2m$ small (local) limit cycles in the vicinity of two focus points and several large (global) limit cycles enclosing all the small limit cycles. The method of normal forms is employed to prove the existence of the small limit cycles and numerical simulation is used to show the existence of large limit cycles.

Keywords: Hilbert's 16th problem; Liénard equation; limit cycles; normal form.

1. Introduction

It has been more than one hundred years since Hilbert [1902] presented the well-known 23 mathematical problems to the Second International Congress of Mathematicians in 1900. Great advances inspired by the famous address have been achieved in many different mathematical areas. However, two of the 23 problems remain unsolved, one of them is the 16th problem named as the *Problem of the topology of algebraic curves and surfaces*. This problem includes two parts. Roughly speaking, the first part is to investigate the relative positions of separate branches of algebraic curves in vector fields. The second part of the problem, on the other hand, is to consider the least upper bound of the number of limit cycles and their relative locations in polynomial vector fields. This part is related to differential equations and dynamical systems. Generally, the second part of the problem is the content of the Hilbert's 16th problem.

The second part of Hilbert's 16th problem was recently reformulated by Smale [1998], as one of the 18 challenging mathematical problems for the 21st century. To be more specific, consider the following planar system:

$$\dot{x} = P_n(x, y), \quad \dot{y} = Q_n(x, y), \tag{1}$$

where the dot denotes differentiation with respect to time, t, and P_n and Q_n represent nth-degree polynomials of x and y. Then, the second part of Hilbert's 16th problem can be stated as follows [Smale, 1998]: Find the upper bound $K = H(n) \le n^q$ on the number of limit cycles that the system can have, where q is a universal constant. In the same article, Smale described a simplified version of Hilbert's 16th problem regarding the Liénard equation [Liénard, 1928]:

$$\dot{x} = y - F(x), \quad \dot{y} = -x, \tag{2}$$

where $F(x)$ is a polynomial. Then the problem is to find an upper bound on the number of limit cycles for the simplified Liénard system through the degree of the polynomial function F. Until now, no upper bound has been found even for the simplified Liénard equation.

Although it has not been possible to obtain the uniform upper bound for $H(n)$, various efforts have been made in finding the maximal number of limit cycles and raising the lower bound of Hilbert number $H(n)$ for general planar polynomial systems or for individual degree of systems. This way people hope to get close to the estimation of the upper bound of $H(n)$. Nevertheless, even for estimating the lower bound of $H(n)$ it is generally a very difficult problem, in particular, for determining large (global) limit cycles. For recent progress on the research of Hilbert's 16th problem, readers are referred to a survey article [Li, 2003] and more references therein.

When the study on Hilbert's 16th problem is restricted to the neighborhood of isolated fixed points, the problem is reduced to consider degenerate Hopf bifurcations. In the past 50 years, many research results have been obtained on the local problem (e.g. see [Bautin, 1952; Kukles, 1944; Li & Liu, 1991; Liu & Li, 1989; Malkin, 1964; Han, 1999, 2002; Zhang *et al.*, 2004]). In the last two decades, much progress on finite cyclicity near a fine focus point or a homoclinic loop has been achieved. For a quadratic system, Bautin [1952] proved that the maximal number of small limit cycles is three. For cubic order systems, the best results obtained recently are twelve limit cycles [Yu, 2002; Yu & Han, 2004, 2005a, 2005b].

In this paper, particular attention is focused on a class of Liénard equation in which $f(x)$ is an even polynomial function with degree $2m$, while $g(x)$ is a third-degree, odd polynomial function. In phase space, the system has three fixed points, one saddle point at the origin and two linear centers which are symmetric about the origin. It will be shown that the system can have $2m$ small limit cycles in the vicinity of two focus points and several large limit cycles enclosing all the small limit cycles.

The key step in finding the number of limit cycles of a system in the neighborhood of a fixed point (which is a linear center) is to compute the focus values of the point. This is equivalent to calculate the normal form of the system associated with Hopf singularity. Many methods have been developed for computing normal forms with computer algebra systems such as Maple, Mathematica, Reduce, etc. Among various methods, a perturbation technique [Yu, 1998] has been proved computationally efficient, which combines normal form computation with center manifold reduction to generate a unified approach. This perturbation technique will be used to prove the existence of small limit cycles. Numerical simulations, on the other hand, will be employed to show the existence of large limit cycles.

The rest of the paper is organized as follows. In the next section, the generalized Liénard equation is presented. A particular case of the Liénard equation for $m = 5$ is considered in detail in Sec. 3 to show the existence of 13 limit cycles, and the results for other values of m, $1 \le m \le 10$, are summarized in Sec. 4. Finally, conclusion is drawn in Sec. 5.

2. The Liénard Equation

In this section, we consider the Liénard equation — a simplified version of Hilbert's 16th problem. Most of the early history in the theory of limit cycles was stimulated by practical problems displaying periodic behavior. For example, in 1877 Rayleigh derived a differential equation to describe the oscillation of a violin string [Rayleigh, 1945] in the form of

$$\ddot{x} + \epsilon\left(\frac{1}{3}\,\dot{x}^2 - 1\right)\dot{x} + x = 0, \tag{3}$$

where ϵ is a small perturbation parameter. Following the invention of the triode vacuum tube, which was able to produce stable self-excited oscillations of constant amplitude, van der Pol [1926] used the following differential equation to describe this phenomenon:

$$\ddot{x} + \epsilon(x^2 - 1)\dot{x} + x = 0. \tag{4}$$

Perhaps the most famous class of differential equations, which is a generalization of Eq. (4), are those first investigated by Liénard [1928], given by Eq. (2):

$$\ddot{x} + f(x)\dot{x} + g(x) = 0.$$

Letting $\dot{x} = y$ in the above equation yields the system described in phase plane:

$$\begin{aligned} \dot{x} &= y, \\ \dot{y} &= -g(x) - f(x)y. \end{aligned} \tag{5}$$

Further, let $y = \tilde{y} - F(x)$, where $F(x) = \int_0^x f(s)ds$. Then we have the following equivalent system:

$$\begin{aligned} \dot{x} &= y = \tilde{y} - F(x), \\ \dot{\tilde{y}} &= \dot{y} + \frac{dF}{dx}\dot{x} = -g(x) - f(x)y + f(x)y \\ &= -g(x). \end{aligned} \tag{6}$$

It is seen that Eq. (2) is a special case of system (6) when $g(x) = x$.

Let $\hat{H}(m, n)$ be the maximum number of small-amplitude limit cycles of system (2), where m and n are the degrees of f and g, respectively. Then the existing results for the Liénard system (2) are summarized in Table 1 [Lynch & Christopher, 1999]. Note that the numbers given in this table are symmetric with respect to f and g [Lloyd & Pearson, 2002], i.e. $\hat{H}(m, n) = \hat{H}(n, m)$. Thus, one only needs to prove for the cases $m \geq n$. It should be pointed out that the notation $\hat{H}(m, n)$ denotes the maximal number of small limit cycles which may exist in the vicinity of the origin. It does not include global (large) limit cycles, nor contain other local (small) limit cycles which may appear in the neighborhood of other nonzero focus points.

For certain, let

$$\begin{aligned} F(x) &= a_1 x + a_2 x^2 + a_3 x^3 + \cdots \\ g(x) &= b_1 x + b_2 x^2 + b_3 x^3 + b_4 x^4 + \cdots \end{aligned} \tag{7}$$

where $b_1 > 0$. If the attention is focused on the dynamic behavior of the system in the vicinity of the origin, then one may introduce a local coordinate transformation [Lynch & Christopher, 1999] to obtain

$$\begin{cases} \dot{u} = y - (A_1 u + A_2 u^2 + A_3 u^3 + A_4 u^4 \\ \qquad + A_5 u^5 + \cdots), \\ \dot{y} = -u, \end{cases} \tag{8}$$

where $A_1 = a_1$, $A_2 = a_2$, and other A_i's are given explicitly in terms of a_i's and b_i's.

It is easy to see from Eq. (8) that the origin $(y, u) = (0, 0)$ is a unique fixed point — a linear center. Further, one can apply the Maple program developed in [Yu, 1998] to system (8) to obtain the normal form given in polar coordinates (see Eqs. (16) and (17) in the next section) with the following focus values:

$$\begin{aligned} v_0 &= -A_1, \\ v_1 &= -\frac{3}{8} A_3, \\ v_2 &= -\frac{5}{16} A_5 - \frac{5}{24} A_2^2 A_3, \end{aligned}$$

Table 1. The values of $\hat{H}(m, n)$ for the generalized Liénard systems associated with the origin when f and g are of varying degrees.

	13	6	9	10										
	12	6	8	10										
	11	5	7	8										
	10	5	7	8										
	9	4	6	8	9									
	8	4	5	6	9									
deg(f)	7	3	5	6	8									
	6	3	4	6	7									
	5	2	3	4	6	6								
	4	2	3	4	4	6	7	8	9	9				
	3	1	2	2	4	4	6	6	6	8	8	8	10	10
	2	1	1	2	3	3	4	5	5	6	7	7	8	9
	1	0	1	1	2	2	3	3	4	4	5	5	6	6
		1	2	3	4	5	6	7	8	9	10	11	12	13
		deg(g)												

$$
\begin{aligned}
v_3 &= -\frac{35}{128}A_7 - \frac{205}{1152}A_4^2 A_5 \\
&\quad - \left(\frac{1885}{13824}A_4^2 + \frac{2}{3}A_2 A_4 + \frac{999}{8192}A_3^2\right)A_3, \\
v_4 &= -\frac{63}{256}A_9 - \frac{413}{2304}A_2^2 A_7 \\
&\quad - \left(\frac{47}{96}A_2 A_4 + \frac{2115}{4096}A_3^2 + \frac{4297}{41472}A_2^4\right)A_5 \\
&\quad - \left(\frac{141}{160}A_2 A_6 + \frac{149}{240}A_4^2 + \frac{1093}{1152}A_2^3 A_4 \right. \\
&\quad \left. + \frac{20599}{49152}A_2^2 A_3^2 + \frac{109483}{1244160}A_2^6\right)A_3, \\
&\vdots
\end{aligned}
\tag{9}
$$

It follows from Eq. (9) that

$$
\begin{aligned}
&v_0 = v_1 = v_2 = v_3 = 0,\ v_4 \neq 0 \\
&\Leftrightarrow A_1 = A_3 = A_5 = A_7 = 0,\ A_9 \neq 0.
\end{aligned}
$$

In general, one can show that

$$
\begin{aligned}
&v_0 = v_1 = v_2 = \cdots = v_{k-1} = 0,\ v_k \neq 0 \\
&\Leftrightarrow A_1 = A_3 = A_5 = \cdots = A_{2k-1} = 0,\ A_{2k+1} \neq 0.
\end{aligned}
$$

Therefore, in order for system (8) or (2) to have k small limit cycles around the origin, it requires that $v_0 = v_1 = v_2 = \cdots = v_{k-1} = 0$, but $v_k \neq 0$, or $A_1 = A_3 = A_5 = \cdots = A_{2k-1} = 0$, but $A_{2k+1} \neq 0$. For example, when $A_1 = 0$, but $A_3 \neq 0$, then system (8) or (2) has maximal one limit cycle around the origin; when $A_1 = A_3 = 0$, $A_5 \neq 0$, then system (8) or (2) has maximal two limit cycles in the neighborhood of the origin; etc. Since the coefficients A_i's are given in terms of a_i's and b_i's, one needs to determine the values of a_i's and b_i's to satisfy the necessary conditions. Further, based on the sufficient conditions given in Theorems 1 and 2 (see the next section), we can apply appropriate perturbations to obtain exact k limit cycles.

In this paper, we shall pay particular attention to a special class of the Liénard equation and investigate the small limit cycles arising form nonzero Hopf critical points and large limit cycles as well. This special class of the Liénard system is described as follows:

$$
\begin{aligned}
\dot{x} &= y, \\
\dot{y} &= -\frac{1}{2}b^2 x(x^2 - 1) - y\sum_{i=0}^{m} a_i x^{2i},
\end{aligned}
\tag{10}
$$

where $b \neq 0$ and a_i's are real coefficients. Equation (9) has three fixed points: $(0, 0)$ and $(\pm 1, 0)$. It is easy to use a linear analysis to show that the origin $(0, 0)$ is a saddle point (with eigenvalues $(1/2)(-a_0 \pm \sqrt{a_0^2 + 2b^2})$). In order to have the two fixed points $(\pm 1, 0)$ being linear centers, the following condition:

$$
\sum_{i=0}^{m} a_i = 0 \quad \text{or} \quad a_0^* = -\sum_{i=1}^{m} a_i, \tag{11}
$$

must be satisfied. The notation * denotes the critical value of the coefficient. Then the eigenvalues of the Jacobian of system (9) evaluated at $(\pm 1, 0)$ are $\pm |b| i$. What we want to do is, for a given m, to choose appropriate values of a_i's such that system (10) has maximal limit cycles in the neighborhood of the two fixed points $(\pm 1, 0)$, and then to further consider large limit cycles. We shall present a detailed analysis for the case $m = 5$ in the next section and then summarize the results for other cases $1 \leq m \leq 10$ in Sec. 4.

Before considering the particular case $m = 5$, we shall show that the coefficient b does not affect the results. In other words, different values of b (as long as they are not equal to zero) do not change the number of limit cycles. To show this, first introduce the following scalings:

$$
a_i \Rightarrow b a_i, \quad i = 0, 1, \ldots, m. \tag{12}
$$

Then apply the transformation, given by

$$
x = \pm 1 + u, \quad y = bv, \tag{13}
$$

and, in addition, the time scaling

$$
\tau = bt \tag{14}
$$

into system (10) to obtain

$$
\begin{aligned}
\frac{du}{d\tau} &= v, \\
\frac{du}{d\tau} &= -u - \frac{3}{2}u^2 - \frac{1}{2}u^3 - v(2u + u^2) \\
&\quad \times \left\{ \sum_{i=1}^{m} a_i + \sum_{i=2}^{m} a_i (1+u)^2 + \sum_{i=3}^{m} a_i (1+u)^3 \right. \\
&\quad + \cdots + (a_{m-1} + a_m)(1+u)^{2m-4} \\
&\quad \left. + a_m (1+u)^{2m-2} \right\},
\end{aligned}
\tag{15}
$$

where condition (11) has been used. The Jacobian of system (15) evaluated at $(u, v) = (0, 0)$ (i.e. at

$(x, y) = (\pm 1, 0)$) is now in the Jordan canonical form. The above procedure shows that the coefficient b can be chosen as any nonzero real values, which does not affect the qualitative behavior of the system. In particular, it does not change the number of limit cycles. Thus, without loss of generality, we assume $b = 1$, and so $\tau = t$, in the rest of the paper.

3. Thirteen Limit Cycles in System (10) for $m = 5$

In this section, we will prove that the Liénard equation (10) for $m = 5$ (i.e. $\deg(f) = 10$) can have thirteen limit cycles, among them ten are small limit cycles and three are big limit cycles. First we shall give two sufficient conditions for the existence of small amplitude limit cycles. Then we shall use the method of normal forms and appropriate perturbations to obtain exact ten small limit cycles. Finally, we will employ numerical simulations to show the existence of three large limit cycles.

3.1. *Sufficient conditions for existence of small limit cycles*

Since we do not intend to discuss normal form computation in this paper, we assume that the normal form for the general system (1) has been obtained in the polar coordinates as follows (interested readers can find the details of normal form computation in [Yu, 1998]):

$$\dot{r} = r(v_0 + v_1 r^2 + v_2 r^4 + \cdots + v_k r^{2k}), \tag{16}$$
$$\dot{\theta} = \omega + t_1 r^2 + t_2 r^4 + \cdots + t_k r^{2k}, \tag{17}$$

up to $(2k+1)$th order term, where both v_k and t_k are expressed in terms of the original system's coefficients. v_k is called the kth-order focus value of the Hopf-type critical point (the origin).

The basic idea of finding k small limit cycles around the origin is as follows: First, find the conditions such that $v_1 = v_2 = \cdots = v_{k-1} = 0$ (v_0 is automatically satisfied at the critical point), but $v_k \neq 0$, and then perform appropriate small perturbations to prove the existence of k limit cycles. This indicates that the procedure for finding multiple small limit cycles involves two steps: computing the focus values (i.e. computing the normal form) and solving the coupled nonlinear polynomial equations: $v_1 = v_2 = \cdots = v_{k-1} = 0$. In the following, we give two theorems for sufficient conditions of the existence of small amplitude limit cycles. (The proof can be found in [Han *et al.*, 2004; Yu & Han, 2004, 2005a, 2005b].)

Theorem 1. *If the focus values v_i in Eq. (16) satisfy the following conditions*:

$$v_i v_{i+1} < 0 \quad \text{and} \quad |v_i| \ll |v_{i+1}| \ll 1, \quad \text{for } i = 0, 1, 2, \ldots, k-1,$$

then the polynomial equation given by $\dot{r} = 0$ in Eq. (16) has k positive real roots of r^2, and thus the original system has k limit cycles.

In many cases, v_j depends on k parameters:

$$v_j = v_j(c_1, c_2, \ldots, c_k), \quad j = 0, 1, \ldots, k, \tag{18}$$

and at the critical point $(c_1, c_2, \ldots, c_k) = (c_{1c}, c_{2c}, \ldots, c_{kc})$, $v_j = 0$, $j = 0, 1, \ldots, k$. One can then perturb these parameters as $c_i = c_{ic} + \epsilon_i$, $i = 1, 2, \ldots, k$ to obtain k limit cycles. In this case, the following theorem is more convenient in applications.

Theorem 2. *Suppose that the condition (18) holds, and further assume that*

$$v_k(c_{1c}, c_{2c}, \ldots, c_{kc}) \neq 0,$$
$$v_j(c_{1c}, c_{2c}, \ldots, c_{kc}) = 0, \quad j = 0, 1, \ldots, k-1 \quad \text{and}$$
$$\det\left[\frac{\partial(v_0, v_1, \ldots, v_{k-1})}{\partial(c_1, c_2, \ldots, c_k)}(c_{1c}, c_{2c}, \ldots, c_{kc})\right] \neq 0. \tag{19}$$

Then for any given $\epsilon_0 > 0$, there exist $\epsilon_1, \epsilon_2, \ldots, \epsilon_k$ and $\delta > 0$ with $|\epsilon_j| < \epsilon_0, j = 1, 2, \ldots, k$ such that equation $\dot{r} = 0$ has exactly k real positive roots of r^2, and thus the corresponding original dynamical system has exactly k limit cycles in a δ-ball with the center at the origin.

3.2. *Existence of ten small limit cycles*

When $m = 5$, system (10) becomes

$$\dot{x} = y,$$
$$\dot{y} = -\frac{1}{2}x(x^2 - 1) - (a_0 + a_2 x^2 + a_4 x^4 + a_6 x^6 + a_8 x^8 + a_{10} x^{10})y, \tag{20}$$

and the condition given in (11) is

$$a_0^* = -(a_2 + a_4 + a_6 + a_8 + a_{10}). \tag{21}$$

The transformed system (15) for $m = 5$ can be rewritten as

$$\dot{u} = v,$$
$$\dot{v} = -u - \frac{3}{2}u^2 - 2(a_2 + 2a_4 + 3a_6 + 4a_8 + 5a_{10})uv$$

$$
\begin{aligned}
&-\frac{1}{2}u^3-(a_2+6a_4+15a_6+28a_8+45a_{10})u^2v\\
&-4(a_4+5a_6+14a_8+30a_{10})u^3v-(a_4+15a_6\\
&+70a_8+210a_{10})u^4v-2(3a_6+28a_8\\
&+128a_{10})u^5v-(a_6+28a_8+210a_{10})u^6v\\
&-8(a_8+15a_{10})u^7v-(a_8+45a_{10})u^8v\\
&-10a_{10}u^9v-a_{10}u^{10}v. \qquad (22)
\end{aligned}
$$

Note that the zero order focus value of system (20) associated with the fixed points $(\pm 1, 0)$ is given by

$$v_0 = -(a_0+a_2+a_4+a_6+a_8+a_{10}). \qquad (23)$$

To obtain the focus values v_i $(i \geq 1)$, employing the Maple program, developed in [Yu, 1998] for computing the normal forms of Hopf and generalized Hopf bifurcations, into system (22) yields

$$v_1 = \frac{1}{4}(a_2-3a_6-8a_8-15a_{10}). \qquad (24)$$

Setting $v_1 = 0$ results in

$$a_2^* = 3a_6+8a_8+15a_{10}. \qquad (25)$$

Then, v_2 can be found as

$$v_2 = \frac{1}{4}(a_4+5a_6+10a_8+10a_{10}). \qquad (26)$$

Hence, letting $v_2 = 0$ leads to

$$a_4^* = -(5a_6+10a_8+10a_{10}). \qquad (27)$$

Then, under the conditions (23), (25) and (27), one similarly obtains

$$v_3 = -\frac{5}{16}(a_6-14a_{10}), \qquad (28)$$

which, in turn, yields

$$a_6^* = 14a_{10} \qquad (29)$$

in order to have $v_3 = 0$. Similarly, one may find

$$v_4 = -\frac{7}{16}(a_8+9a_{10}), \qquad (30)$$

and thus

$$a_8^* = -9a_{10}, \qquad (31)$$

under which $v_4 = 0$. For convenience, we rewrite the critical values of the coefficients in a reverse order as follows:

$$
\begin{aligned}
a_8^* &= -9a_{10},\\
a_6^* &= 14a_{10},\\
a_4^* &= -(5a_6+10a_8+10a_{10}),\\
a_2^* &= 3a_6+8a_8+15a_{10},\\
a_0^* &= -(a_2+a_4+a_6+a_8+a_{10}),
\end{aligned} \qquad (32)
$$

under which $v_i = 0$, $i = 0, 1, 2, 3, 4$.

Finally, for the critical parameter values given in Eq. (32), higher order focus values are obtained as

$$
\begin{aligned}
v_5 &= \frac{21}{32}a_{10},\\
v_6 &= a_{10}\left(\frac{9}{16}+\frac{464}{3}a_{10}^2\right),\\
v_7 &= a_{10}\left(\frac{4449}{4096}-439a_{10}^2+\frac{679616}{27}a_{10}^4\right),\\
v_8 &= a_{10}\left(\frac{17753}{8192}+\frac{74641}{96}a_{10}^2-\frac{2849296}{15}a_{10}^4\right.\\
&\quad\left.+\frac{6911524864}{2025}a_{10}^6\right),\\
&\ \ \vdots
\end{aligned} \qquad (33)
$$

It can be shown that $v_i = a_{10}h_i(a_{10}^2)$ for $i \geq 5$, where $h_i(a_{10}^2)$ represents a polynomial of a_{10}^2. Thus, setting $a_{10} = 0$ yields $v_5 = v_6 = v_7 = \cdots = 0$, leading to a center. So assume that $a_{10} \neq 0$, then $v_6 \neq 0$, and $v_7 \neq 0$ since $v_7 = 0$ has no real solution for a_{10}. When a_{10} is chosen such that $|a_{10}| \ll 1$, v_5 dominates the dynamical behavior of the system in the vicinity of the origin.

Next, we want to perform appropriate perturbations to the critical parameter values to obtain exact five limit cycles around each of the two fine focus points $(\pm 1, 0)$. Without loss of generality, assume $0 < a_{10} \ll 1$, then we need to find perturbations to a_8, a_6, a_4, a_2 and a_0 such that

$$0 < -v_0 \ll v_1 \ll -v_2 \ll v_3 \ll -v_4 \ll v_5 \ll 1.$$

Note that all the focus values v_i, $i = 0, 1, 2, 3, 4, 5$ are given in linear forms of the coefficients a_i. Further, consider the back order perturbations one by one: First on a_8 for v_4, then on a_6 for v_3, and on a_4 for v_2, on a_2 for v_1, and finally on a_0 for v_0. Therefore, the perturbation procedure is straightforward. Since $\partial v_4/\partial a_8 = -(7/16) < 0$, one may perturb $a_8 = -9a_{10}$ to $a_8 = -9a_{10} + \epsilon_1$ $(0 < \epsilon_1 \ll 1)$, and thus $v_4 = -(7/16)\epsilon_1 < 0$. Similarly, we may let $a_6 = 14a_{10} - \epsilon_2$ $(0 < \epsilon_2 \ll \epsilon_1)$, and thus $v_3 = -(5/16)\epsilon_2$. This procedure can be processed until a_0 for v_0. The main results of this paper are summarized in the following theorem.

Theorem 3. *Given the Liénard equation (20) which has a saddle point at the origin and a pair of symmetric fine focus points at* $(x, y) = (\pm 1, 0)$, *under the condition* $b \neq 0$ *and* $a_0 = -(a_2+a_4+a_6+a_8+a_{10})$. *Further, take* $b = 1$, *and perturb* a_8, a_6, a_4, a_2

and a_0 *as*

$$\begin{aligned} a_8 &= a_8^* + \epsilon_1 = -9a_{10} + \epsilon_1, \\ a_6 &= a_6^* - \epsilon_2 = 14a_{10} - \epsilon_2, \\ a_4 &= a_4^* - \epsilon_3 = 10a_{10} - 10\epsilon_1 + 5\epsilon_2 - \epsilon_3, \\ a_2 &= a_2^* + \epsilon_4 = -15a_{10} + 8\epsilon_1 - 3\epsilon_2 + \epsilon_4, \\ a_0 &= a_0^* + \epsilon_5 = -a_{10} + \epsilon_1 - \epsilon_2 + \epsilon_3 - \epsilon_4 + \epsilon_5, \end{aligned} \tag{34}$$

where $0 < \epsilon_5 \ll \epsilon_4 \ll \epsilon_3 \ll \epsilon_2 \ll \epsilon_1 \ll 1$, *then system* (*20*) *has exactly ten small limit cycles.*

Proof. First note that

$$0 < v_5 = \frac{21}{32} a_{10} \ll 1$$

since $0 < a_{10} \ll 1$. Then for the given perturbation $a_8 = -9a_{10} + \epsilon_1$, we have

$$v_4 = -\frac{7}{16}\epsilon_1,$$

where $0 < \epsilon_1 \ll 1$. Thus, one may choose $0 < \epsilon \ll a_{10} \ll 1$ so that $0 < -v_4 = (7/16)\epsilon_1 \ll (21/32)a_{10} = v_5$.

Similarly, for $a_6 = 14a_{10} - \epsilon_2$, we obtain

$$v_3 = \frac{5}{16}\epsilon_2,$$

where $0 < \epsilon_2 \ll 1$. Therefore, in order to have $0 < v_3 \ll -v_4$, we should choose ϵ_2 such that $0 < \epsilon_2 \ll \epsilon_1$.

Next, for the perturbed parameter values given in Eq. (34), we have

$$v_2 = \frac{1}{4}(a_4 + 5a_6 + 10a_8 + 10a_{10}) = -\frac{1}{4}\epsilon_3.$$

Hence, by choosing $0 < \epsilon_3 \ll \epsilon_2$, one obtains $0 < -v_2 \ll v_3$.

For v_1, we find

$$v_1 = \frac{1}{4}(a_2 - 3a_6 - 8a_8 - 15a_{10}) = \frac{1}{4}\epsilon_4.$$

Then one may select $0 < \epsilon_4 \ll \epsilon_3$ so that $0 < v_1 \ll -v_2$.

Finally, substituting the parameter values given in Eq. (34) into v_0 yields

$$v_0 = -(a_0 + a_2 + a_4 + a_6 + a_8 + a_{10}) = -\epsilon_5.$$

Thus, $0 < -v_0 \ll v_1$ as long as $\epsilon_5 \ll \epsilon_4$.

Summarizing the above perturbation results gives

$$\begin{aligned} 0 < -v_0 = \epsilon_5 \ll v_1 = \frac{1}{4}\epsilon_4 \ll -v_2 = \frac{1}{4}\epsilon_3 \ll v_3 \\ = \frac{5}{16}\epsilon_2 \ll -v_4 = \frac{7}{16}\epsilon_1 \ll v_5 = \frac{21}{32}a_{10} \ll 1, \end{aligned}$$

where $0 < \epsilon_5 \ll \epsilon_4 \ll \epsilon_3 \ll \epsilon_2 \ll \epsilon_1 \ll a_{10} \ll 1$. Therefore, the sufficient conditions given in Theorem 1 are satisfied and so system (20) can have five small amplitude limit cycles near each of the two fine focus points $(\pm 1, 0)$. ∎

To end this subsection, we present a numerical example of choosing proper perturbations to have ten small limit cycles. Let $b = 1$ and

$$a_{10} = 0.002 \Rightarrow v_5 = 0.13125 \times 10^{-2}, \tag{35}$$

and further choose the following perturbations:

$$\begin{aligned} \epsilon_1 &= 0.1 \times 10^{-4} \Rightarrow v_4 = -0.4375 \times 10^{-5}, \\ \epsilon_2 &= 0.1 \times 10^{-7} \Rightarrow v_3 = 0.3125 \times 10^{-8}, \\ \epsilon_3 &= 0.1 \times 10^{-11} \Rightarrow v_2 = -0.25 \times 10^{-12}, \\ \epsilon_4 &= 0.1 \times 10^{-16} \Rightarrow v_1 = 0.25 \times 10^{-17}, \\ \epsilon_5 &= 0.1 \times 10^{-23} \Rightarrow v_0 = -0.1 \times 10^{-23}. \end{aligned} \tag{36}$$

Then, the normal form (16) associated with the fine focus points $(\pm 1, 0)$ up to term r^{11} becomes

$$\begin{aligned} \dot{r} = r(&-0.1 \times 10^{-23} + 0.25 \times 10^{-17} r^2 \\ &- 0.25 \times 10^{-12} r^4 + 0.3125 \times 10^{-8} r^6 \\ &- 0.4375 \times 10^{-5} r^8 + 0.13125 \times 10^{-2} r^{10}), \end{aligned} \tag{37}$$

which, in turn, yields the following five positive roots for r^2:

$$\begin{aligned} r_1^2 &= 0.41732523648679809375743607016 1 \times 10^{-6}, \\ r_2^2 &= 0.11180360424685520982108304364 9 \times 10^{-4}, \\ r_3^2 &= 0.78173661597499891942834483261 5 \times 10^{-4}, \\ r_4^2 &= 0.88604229130114018139910233356 8 \times 10^{-3}, \\ r_5^2 &= 0.23575196947735209409155307760 7 \times 10^{-2}. \end{aligned} \tag{38}$$

So the amplitudes of the five limit cycles are approximately equal to

$$\begin{aligned} r_1 = 0.000646, \quad r_2 = 0.003344, \\ r_3 = 0.008842, \quad r_4 = 0.029766, \\ r_5 = 0.048554. \end{aligned} \tag{39}$$

Under the perturbations given in Eq. (36), the perturbed parameter values are

$$\begin{aligned} a_0 &= -0.0019900009999000009999999, \\ a_2 &= -0.0299200299999999 9, \\ a_4 &= 0.019900049999, \\ a_6 &= 0.02799999, \\ a_8 &= -0.01799, \\ a_{10} &= 0.002, \end{aligned} \tag{40}$$

under which we apply the Maple program [Yu, 1998] to recompute the focus values, given below:

$$
\begin{aligned}
v_0 &= -0.1 \times 10^{-23}, \\
v_1 &= 0.25 \times 10^{-17}, \\
v_2 &= -0.24999874858487645350844377999333338888875 \times 10^{-12}, \\
v_3 &= 0.31248592319463145473698564616776822532047714996127 \times 10^{-8}, \\
v_4 &= -0.43729668984998167395805239671367826480145038363181 \times 10^{-5}, \\
v_5 &= 0.13092188621480516884116851907719947310507220215075 \times 10^{-2}, \\
v_6 &= 0.11201788692745322065172995584472168778163393838020 \times 10^{-2}, \\
v_7 &= 0.21572446829671915961030781924001281001021059005183 \times 10^{-2}, \\
v_8 &= 0.43178136496957954512126359067753972460949294807702 \times 10^{-2}
\end{aligned}
$$

which, in turn, results in the following roots of r^2:

$$
\begin{aligned}
r_1^2 &= 0.417325145871873343198217715836 \times 10^{-6}, \\
r_2^2 &= 0.111803557370515325752354199181 \times 10^{-4}, \\
r_3^2 &= 0.781731053867996798394154100054 \times 10^{-4}, \\
r_4^2 &= 0.885965623364635521752016958065 \times 10^{-3}, \\
r_5^2 &= 0.235689632885664418839052249864 \times 10^{-2}, \\
r_6^2 &= -0.723249613594848097066617028472, \\
r_{7,8}^2 &= 0.110150965372161277030407639683 \\
&\quad \pm 0.638988085546118611924228836755i. \quad (41)
\end{aligned}
$$

The first five positive roots are identical to that given in Eq. (38) at least up to six digit points, indicating that higher order focus values due to the perturbations do not affect the solutions of the limit cycles. This indeed shows that ten small limit cycles exist in the neighborhood of the two fine focus points $(\pm 1, 0)$.

For the parameter values given in Eq. (40), the phase portrait for system (20) obtained from computer simulations is shown in Fig. 1, where ten small limit cycles are depicted near the points $(\pm 1, 0)$. It should be pointed out that the trajectories which are not near the two focus points $(\pm 1, 0)$ can be obtained quite accurately using numerical simulations. However, one cannot obtain the computer simulation results for the small limit cycles since the accuracy of some parameters is higher than the machine precision. That is why one must employ certain theoretical approach (like the one presented in this paper) to prove the existence of small limit cycles. In fact, in the neighborhood of a highly degenerate focus point, trajectories behave like around centers, as shown in Fig. 1. The stabilities of these small limit cycles can be easily determined by the signs of the focus values. For convenience, let these small limit cycles be named, from the smallest to the largest, as l_1, l_2, l_3, l_4 and l_5, respectively. Since $v_0 < 0$, the focus points $(\pm 1, 0)$ are stable. Then the smallest limit cycle l_1 is unstable, and thus l_2 is stable, and so on. It can be observed from Fig. 1 that besides the small limit cycles, there also exist large limit cycles. It seems that there are at least two large limit cycles. In the next subsection, we shall show that there actually exist three large limit cycles.

3.3. *Existence of three large limit cycles*

In this subsection, we shall explore numerical simulations to investigate the existence of large limit

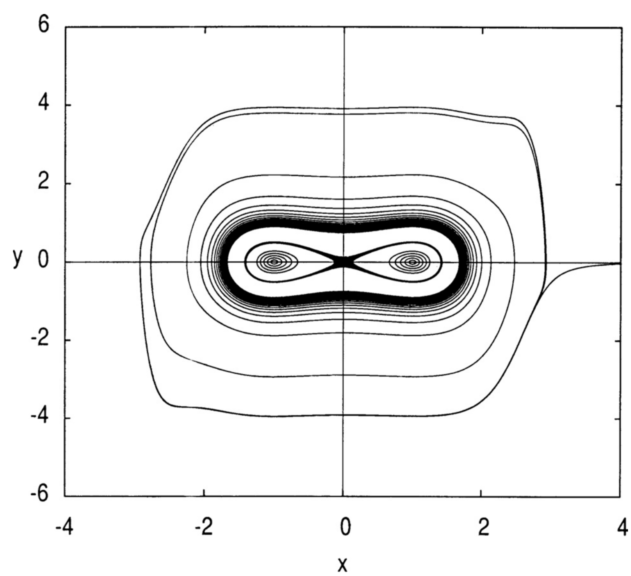

Fig. 1. The phase portrait of system (20) showing ten small limit cycles around the fine focus points $(\pm 1, 0)$ under the perturbed parameter values: $b = 1$, $a_0 = -0.0019900009999000009999999$, $a_2 = -0.0299200299999999$, $a_4 = 0.019900049999$, $a_6 = 0.02799999$, $a_8 = -0.01799$, $a_{10} = 0.002$.

cycles in system (20). Again we use the same parameter values for obtaining small limit cycles, given by Eq. (40). It has been observed from Fig. 1 that large limit cycles do exist. Now we want to show that there are actually three large limit cycles exhibited by system (20) when the parameter values are given by Eq. (40). For convenience, we call the large limit cycles from the largest to the smallest as L_1, L_2 and L_3.

In order to give a comparison, we first present the results obtained from system (20) without perturbations. The unperturbed parameter values are

$$\begin{aligned} a_0 &= -0.002, \quad a_2 = -0.03, \quad a_4 = 0.02, \\ a_6 &= 0.028, \quad a_8 = -0.018, \quad a_{10} = 0.002, \end{aligned} \tag{42}$$

under which $v_i = 0, i = 0, 1, 2, 3, 4$, indicating that the two points $(\pm 1, 0)$ are unstable since the fifth-order focus value, $v_5 = 0.0013125 > 0$. The simulation results are shown in Fig. 2. It seems that there exist three large limit cycles: the outer one is stable while the middle one is unstable [see Fig. 2(a)]. There is a third limit cycle which is stable, as shown in Fig. 2(b). To simulate unstable limit cycles (or in general for any unstable solutions or trajectories), one needs to use reverse time evolution. In other words, negative time steps should be used in simulations. The trajectories starting nearby the two focus points diverge very slowly toward the third large limit cycle (the trajectories nearby the focus points are not shown in Fig. 2(b)). This implies that the unperturbed system does not have small limit cycles around the focus points, as expected.

Now, we investigate the large limit cycles that existed in system (20) with the perturbed

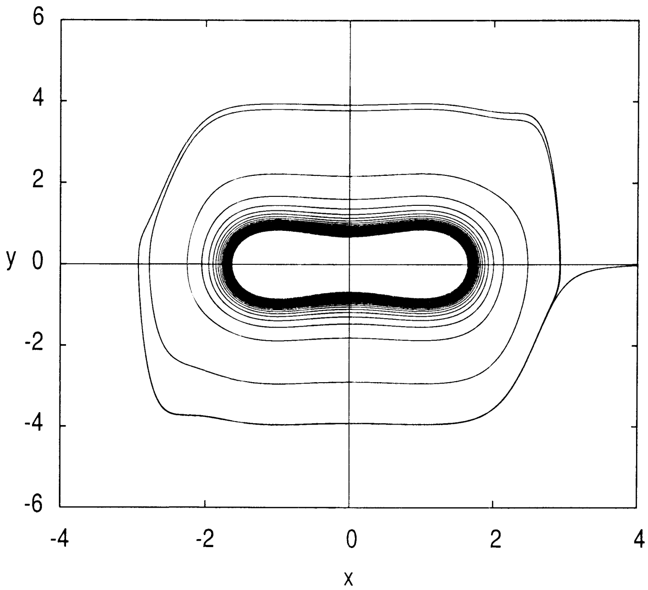

(a)

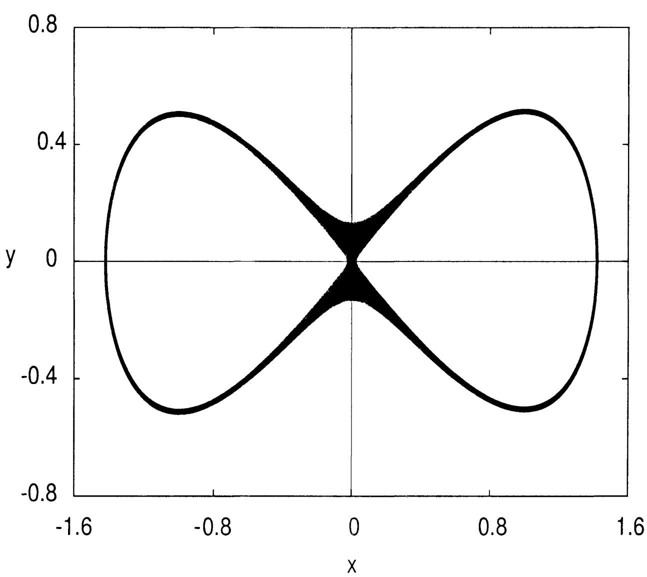

(b)

Fig. 2. The phase portrait of system (20) for the unperturbed parameter values: $b = 1$, $a_0 = -0.002$, $a_2 = -0.03$, $a_4 = 0.02$, $a_6 = 0.028$, $a_8 = -0.018$, $a_{10} = 0.002$: (a) showing two large limit cycles, outer one is stable while the inner one is unstable; (b) showing the trajectories around the fixed points.

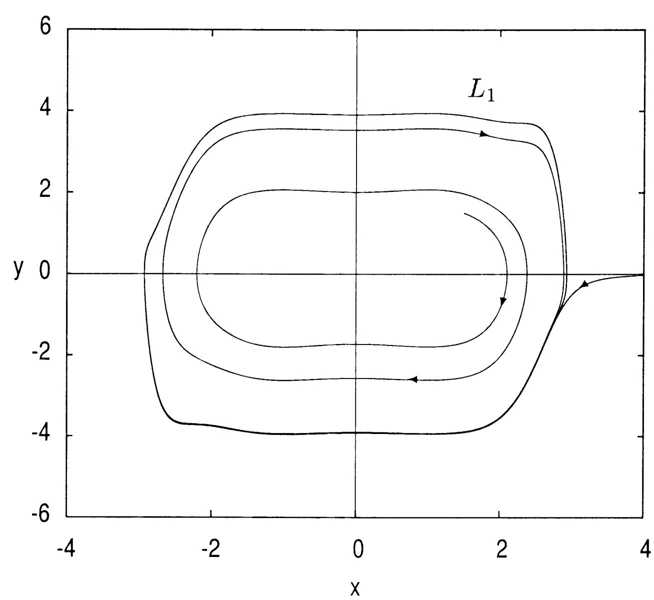

Fig. 3. Trajectories of system (20) converging to the largest limit cycle L_1 as $t \to +\infty$, one from outside with the initial point $(4, 0)$, and the other from inside with the initial point $(1.5, 1.5)$.

parameter values given in Eq. (40). First, consider the largest limit cycle L_1. The numerical simulation result is given in Fig. 3, where two typical trajectories are depicted, one from outside L_1 and the other from inside L_1. Both two trajectories converge to L_1 as $t \to +\infty$. This indicates that the limit cycle L_1 is stable. Then, we know that the limit cycle L_2 should be unstable while the limit cycle L_3 is stable.

Next, consider the limit cycle L_2, which is unstable. The simulation result is shown in Fig. 4. Figure 4(a) demonstrates two trajectories, one from outside L_2 and one from inside L_2, while Fig. 4(b) shows the final state of the trajectories. It is seen that both two trajectories converge to L_2 as $t \to -\infty$, implying that the limit cycle L_2 is unstable, as expected.

Finally, consider the limit cycle L_3, which is stable. The numerical simulation result is shown in Fig. 5. Figure 5(a) depicts two trajectories, one from outside L_3 and one from inside L_3. Both of them converge to the stable limit cycle L_3 as $t \to +\infty$. Figure 5(b) shows the final state of the trajectories. It has been observed that the convergence for this case is much slower than that of the larger limit cycles L_1 and L_2, because this one is close to the degenerate focus points.

Summarizing the above results on the large limit cycles gives the following theorem.

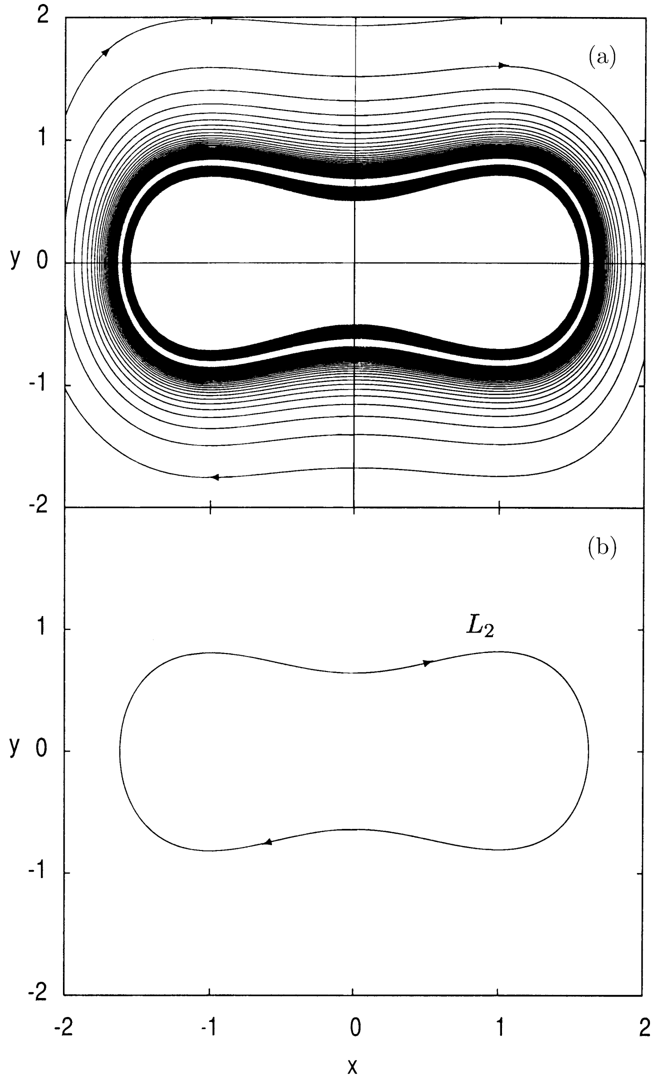

Fig. 4. Trajectories of system (20) converging to the larger limit cycle L_2 as $t \to -\infty$: (a) one from outside with the initial point $(1, 2)$, and the other from inside with the initial point $(0.0, 0.5)$; (b) the final state of the unstable limit cycle.

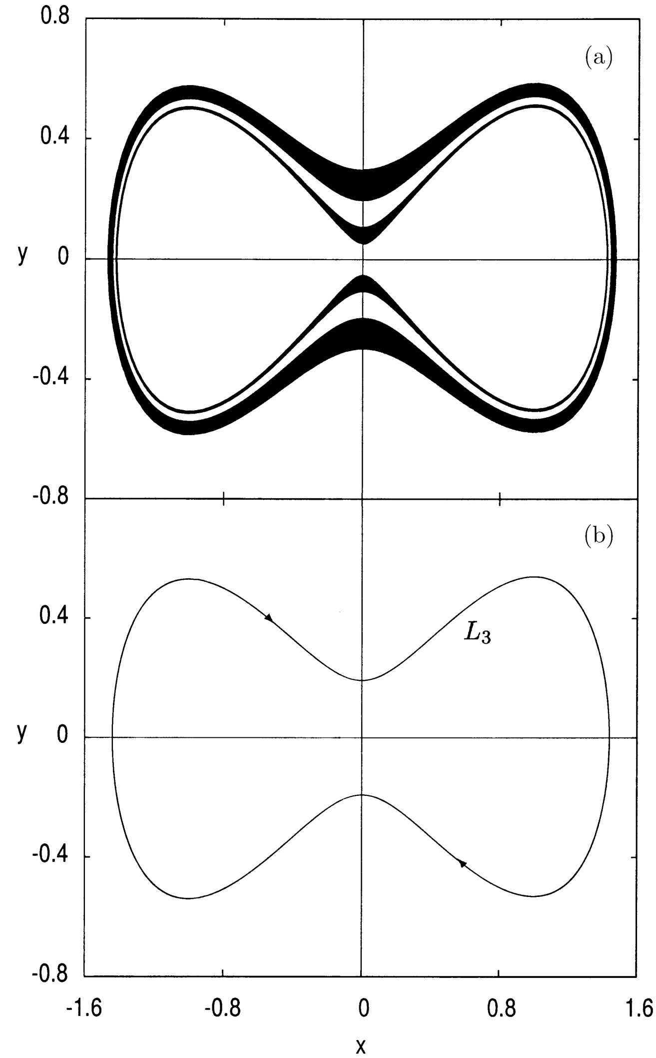

Fig. 5. Trajectories of system (20) converging to the large limit cycle L_3 as $t \to +\infty$: (a) one from outside with the initial point $(0, 0.3)$, and the other from inside with the initial point $(0.0, 0.05)$; (b) the final state of the unstable limit cycle.

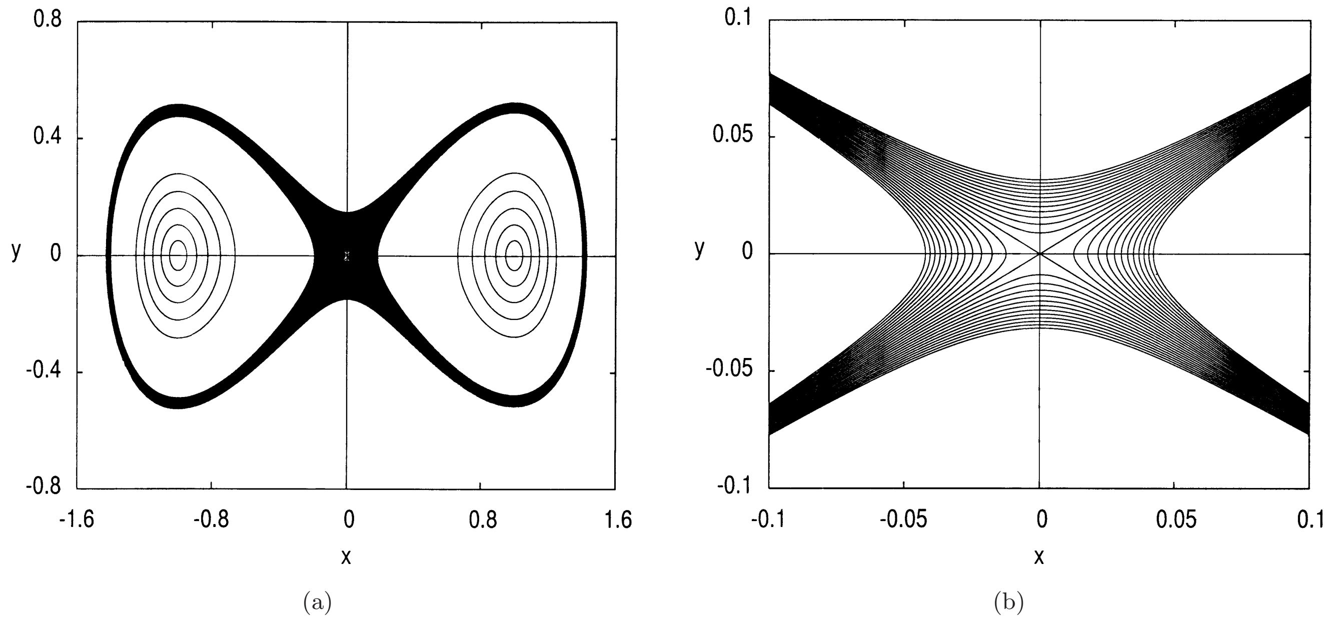

Fig. 6. Trajectories of system (20) around the fixed points: (a) near the two focus points; (b) near the saddle point (the origin).

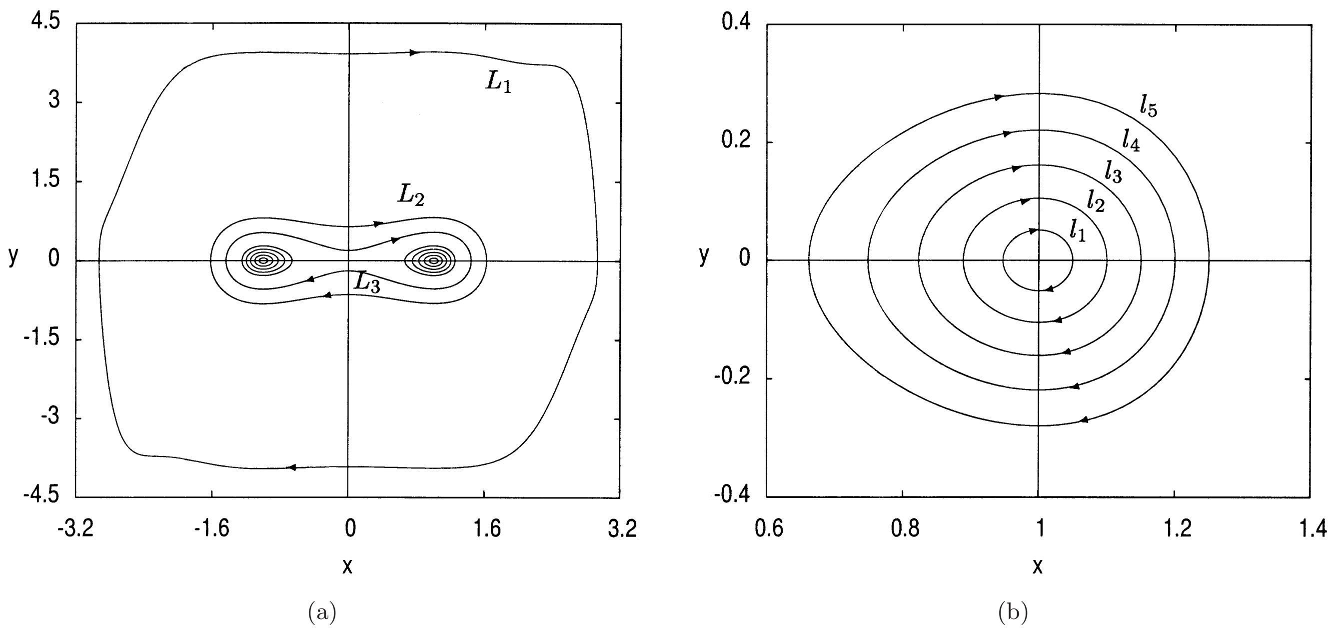

Fig. 7. Thirteen limit cycles of system (20) obtained for parameter values: $b = 1$, $a_0 = -0.00199000999900000999999$, $a_2 = -0.02992002999999999$, $a_4 = 0.019900049999$, $a_6 = 0.02799999$, $a_8 = -0.01799$, $a_{10} = 0.002$, (a) all the 13 limit cycles; (b) the zoom-in area around the focus point $(0, 0)$ having five small limit cycles.

Table 2. Stabilities of the fixed points and limit cycles of Eq. (20).

Saddle Point	Focus Point	Limit Cycle							
$(0, 0)$	$(\pm 1, 0)$	l_1	l_2	l_3	l_4	l_5	L_3	L_2	L_1
U	S	U	S	U	S	U	S	U	S

S = Stable, U = Unstable.

Table 3. Limit cycles in the Liénard system near one focus point and two focus points.

$\deg(f) = k$		1	2	3	4	5	6	7	8	9	10	11	12	13	14	15	16	17	18	19	20
Focus Point $(0, 0)$	Local	1	2	2	4	4	6	6	6	8	8	8	10	10	12	12	12	14	14	14	16
$\frac{1}{2}\deg(f) = m$			1		2		3		4		5		6		7		8		9		10
Focus Points $(\pm 1, 0)$	Local		2		4		6		8		10		12		14		16		18		20
	Global		1		1		2		2		3		3		3		3		4		4

Theorem 4. *Given the Liénard equation (20) with the following parameter values*:

$$b = 1, \quad a_0 = -0.001990009999000009999999,$$
$$a_2 = -0.02992002999999999,$$
$$a_4 = 0.019900049999, \quad a_6 = 0.02799999,$$
$$a_8 = -0.01799 \quad \text{and} \quad a_{10} = 0.002,$$

system (20) has three large limit cycles. The outer and inner ones are stable while the middle one is unstable. The three large limit cycles enclose all the ten small limit cycles.

The simulation results shown in Fig. 6 demonstrate the trajectories around the three fixed points. Figure 6(a) shows the small limit cycles in the vicinity of the two fine focus points $(\pm 1, 0)$, while Fig. 6(b) depicts the behavior of the system near the saddle point $(0, 0)$. Note that the small limit cycles are exaggerated (larger than the true ones) for a clear view, and that the trajectories passing through the saddle point are no longer homoclinic orbits due to the perturbations.

Based on the results given in this section, we conclude that system (20) can have thirteen limit cycles: five small limit cycles surround each of the two focus points and three large limit cycles enclose all the ten small limit cycles, as shown in Fig. 7(a), while Fig. 7(b) is a zoom-in area around the focus point $(1, 0)$ showing five small limit cycles. The stabilities of these limit cycles are given in Table 2.

4. Limit Cycles in the Liénard System (10) for $1 \leq m \leq 10$

The procedure given in the previous section can be used to consider other integer values of m. Since the proofs are similar to that of the case $m = 5$, we will omit the details but present a summary of the results. We have used the method of normal forms to prove that the exact number of the small limit cycles which exist in the neighborhood of the two fine focus points $(\pm 1, 0)$ is $2m$, i.e. $\overline{H}(2m, 3) = 2m$, where $\overline{H}$ is the Hilbert number of the small limit cycles in the vicinity of the two fine focus points. For the local limit cycles around the origin, as shown in Table 1, it has been shown that $\hat{H}(k, 3) = 2[3(k + 2)/8]$, where $[\cdot]$ denotes the maximum integer and $\deg(f) = k$, $k = 2, 3, \ldots, 50$ [Lynch & Christopher, 1999]. The comparison for the above two different cases of local limit cycles is given in Table 3. Obviously, considering the symmetry with two focus points can have more limit cycles.

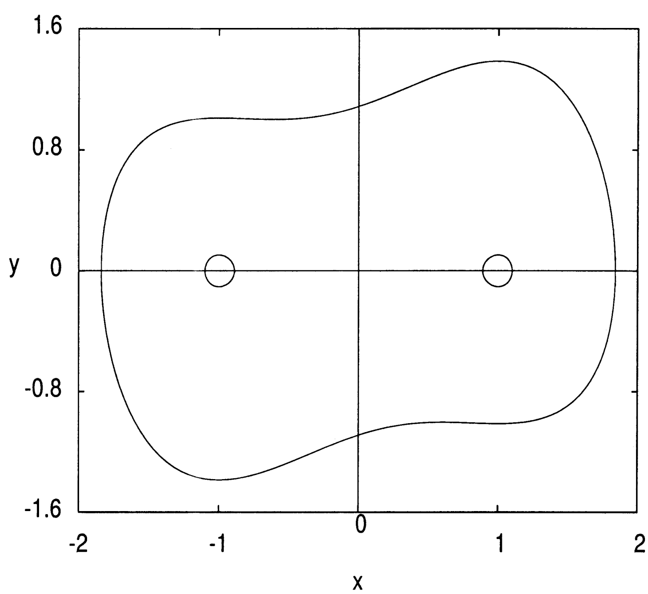

Fig. 8. The phase portrait of system (10) when $m = 1$, showing three limit cycles under the perturbed parameter values: $b = 1$, $a_0 = -0.299$, $a_1 = 0.2$.

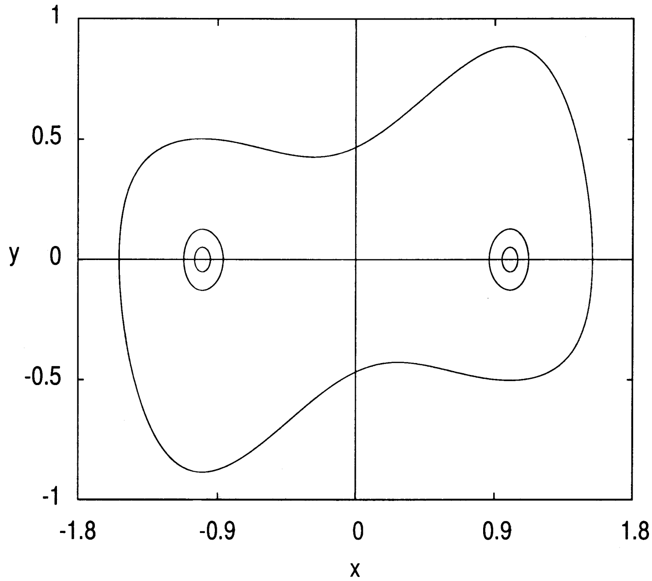

Fig. 9. The phase portrait of system (10) when $m = 2$, showing five limit cycles under the perturbed parameter values: $b = 1$, $a_0 = -0.29002$, $a_1 = -0.01$, $a_2 = 0.3$.

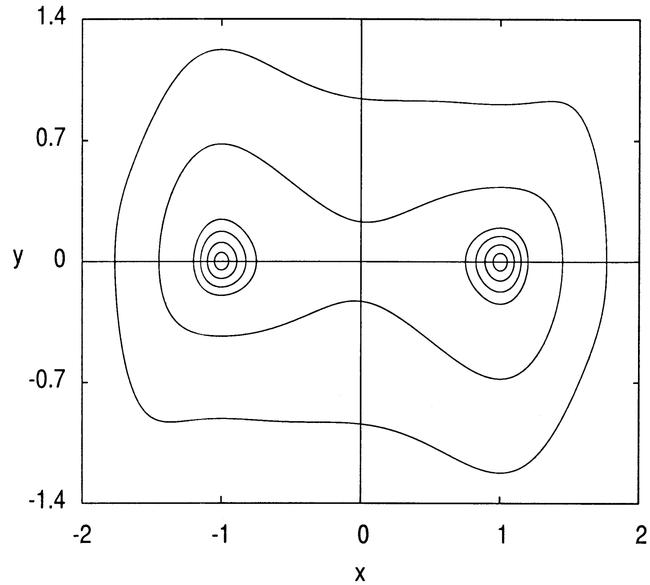

Fig. 11. The phase portrait of system (10) when $m = 4$, showing ten limit cycles under the perturbed parameter values: $b = 1$, $a_0 = 0.09009980001$, $a_1 = 0.7700002$, $a_2 = -0.9501$, $a_3 = -0.01$, $a_4 = 0.1$.

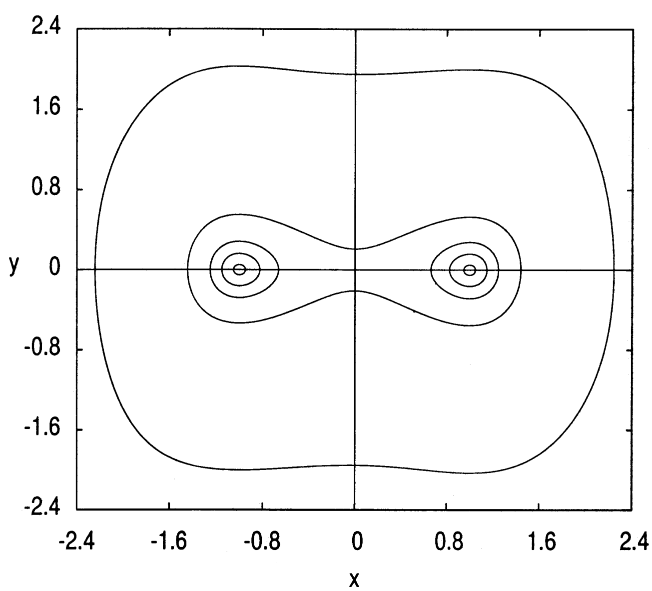

Fig. 10. The phase portrait of system (10) when $m = 3$, showing eight limit cycles under the perturbed parameter values: $b = 1$, $a_0 = 0.0101999$, $a_1 = 0.0598$, $a_2 = -0.09$, $a_3 = 0.02$.

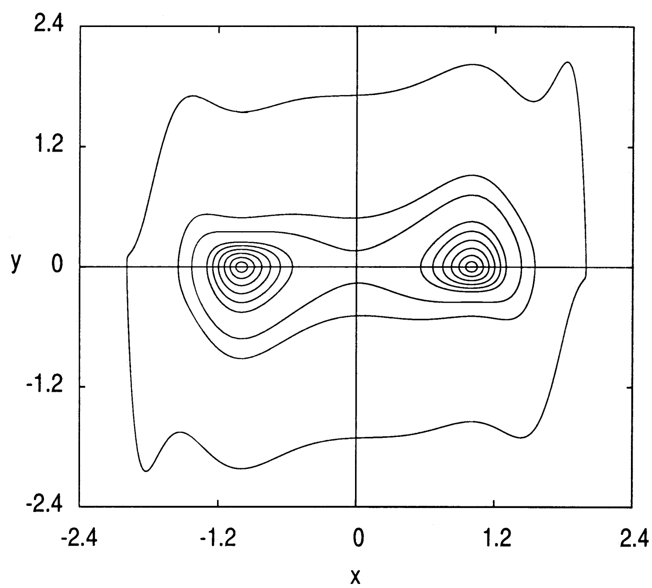

Fig. 12. The phase portrait of system (10) when $m = 6$, showing 15 limit cycles under the perturbed parameter values: $b = 1$, $a_0 = -0.0480199500049999000008$, $a_1 = -1.1701598500000001$, $a_2 = -0.269800249995$, $a_3 = 2.77200005$, $a_4 = -1.33202$, $a_5 = -0.002$, $a_6 = 0.05$.

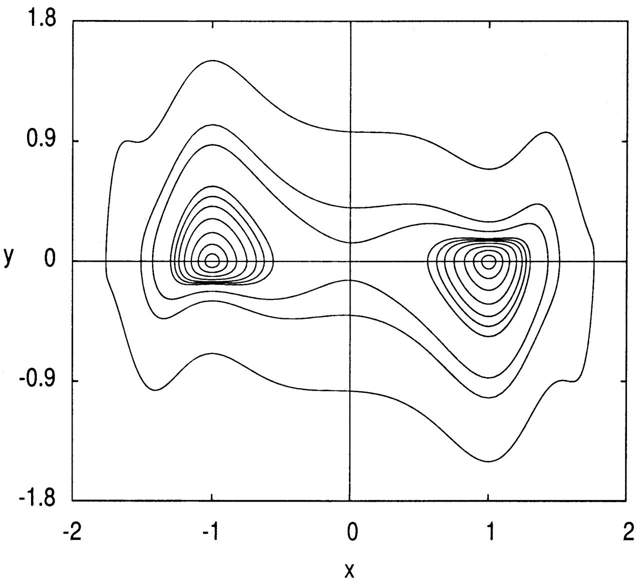

Fig. 13. The phase portrait of system (10) when $m = 7$, showing 17 limit cycles under the perturbed parameter values:

$$b = 1, \quad a_0 = 0.04950099950004999900003999999,$$
$$a_1 = 1.73801499600014999999996,$$
$$a_2 = 2.447490004999750001, \quad a_3 = -6.62201399999995,$$
$$a_4 = 1.3365089995, \quad a_5 = 1.649999,$$
$$a_6 = -0.6495, \quad a_7 = 0.05.$$

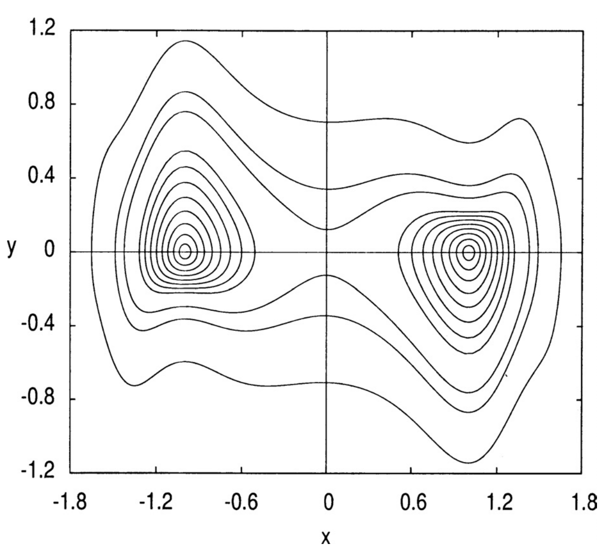

Fig. 14. The phase portrait of system (10) when $m = 8$, showing 19 limit cycles under the perturbed parameter values:

$$b = 1, \quad a_0 = 0.0190099900019999000009999900000001,$$
$$a_1 = 0.92523985001599970000000001,$$
$$a_2 = 2.751050099980000499999, \quad a_4 = -1.826730089998,$$
$$a_5 = 3.48700001, \quad a_6 = -1.02701, \quad a_7 = -0.001,$$
$$a_8 = 0.02.$$

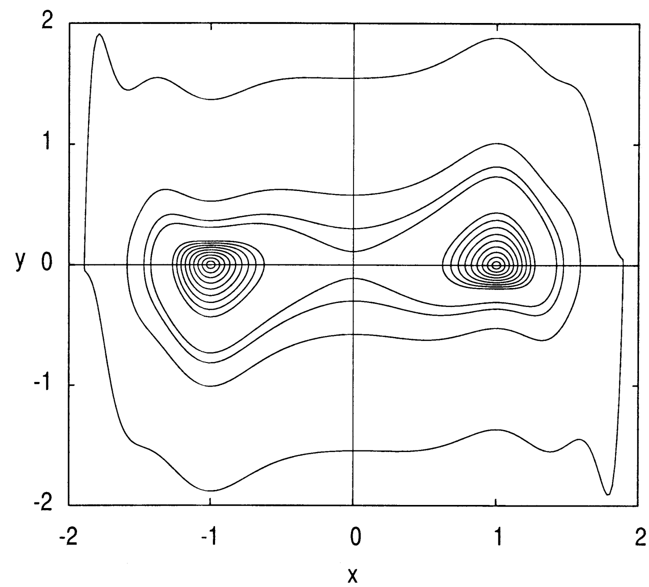

Fig. 15. The phase portrait of system (10) when $m = 9$, showing 19 limit cycles under the perturbed parameter values:

$$b = 1,$$
$$a_0 = -0.00950399200399950000999996000029999999,$$
$$a_1 = -0.60613980805999600002999999999997,$$
$$a_2 = -2.930195959960004999995000004,$$
$$a_3 = 2.408531552055999999999, \quad a_4 = 5.1748922159640005,$$
$$a_5 = -4.972131999996, \quad a_6 = 0.494051992, \quad a_7 = 0.599996,$$
$$a_8 = -0.1695, \quad a_9 = 0.01.$$

For large limit cycles, on the other hand, we apply a fourth-order Rung–Kutta integration scheme to show their existence, as depicted in Figs. 8–16 for $m = 1, 2, 3, 4, 6, 7, 8, 9, 10$. The numbers of the large limit cycles are also shown in Table 3. A careful examination of these numbers seems to suggest that the numbers of the large limit cycles obey the following rule:

$$H^* = \begin{cases} 1 & \text{for } m = 1, \\ p & \text{for } 2^{p-1} + 1 \le m \le 2^p, \\ & \quad p = 1, 2, 3, 4, \ldots \end{cases} \tag{43}$$

In Figs. 8–16, the large limit cycles are truly obtained from computer simulations. However, the small limit cycles are shown just for an illustration since, in particular for larger values of m, they cannot be obtained via computer simulations. They have to be proved using a theoretical approach. In order to present a more accurate information for these small limit cycles, we list the amplitudes of the periodic solutions (obtained from the normal form) below for reference.

$m = 1 : r_1 = 0.01333333$ (see Fig. 8).

$m = 2 : r_1 = 0.01333333, \quad r_2 = 0.02$ (see Fig. 9).

$m = 3 : r_1 = 0.00225219, \quad r_2 = 0.01874441, \quad r_3 = 0.37900340$ (see Fig. 10).

$m = 4 : r_1 = 0.00022449, \quad r_2 = 0.00279562, \quad r_3 = 0.00581885, \quad r_4 = 0.06258961$ (see Fig. 11).

$m = 6 : r_1 = 0.00000394, \quad r_2 = 0.00002551, \quad r_3 = 0.00005344, \quad r_4 = 0.00273615, \quad r_5 = 0.00658136, \quad r_6 = 0.01605414$ (see Fig. 12).

$m = 7 : r_1 = 0.00000153, \quad r_2 = 0.00000381, \quad r_3 = 0.00001508, \quad r_4 = 0.00006981, \quad r_5 = 0.00037915, \quad r_6 = 0.00112468, \quad r_7 = 0.00455979$ (see Fig. 13).

$m = 8 : r_1 = 0.00020429, \quad r_2 = 0.00105575, \quad r_3 = 0.00308633, \quad r_4 = 0.00632467, \quad r_5 = 0.01074805, \quad r_6 = 0.02308772, \quad r_7 = 0.08681535, \quad r_8 = 0.14752576$ (see Fig. 14).

$m = 9 : r_1 = 0.00000017, \quad r_2 = 0.00000084, \quad r_3 = 0.00000312, \quad r_4 = 0.00001282, \quad r_5 = 0.00010222, \quad r_6 = 0.00030878, \quad r_7 = 0.00124938, \quad r_8 = 0.00395682, \quad r_9 = 0.02377763$ (see Fig. 15).

$m = 10 : r_1 = 0.00000001, \quad r_2 = 0.00000002, \quad r_3 = 0.00000077, \quad r_4 = 0.00000285, \quad r_5 = 0.00001212, \quad r_6 = 0.00009727, \quad r_7 = 0.00029989, \quad r_8 = 0.00121941, \quad r_9 = 0.00388862, \quad r_{10} = 0.02342640$ (see Fig. 16).

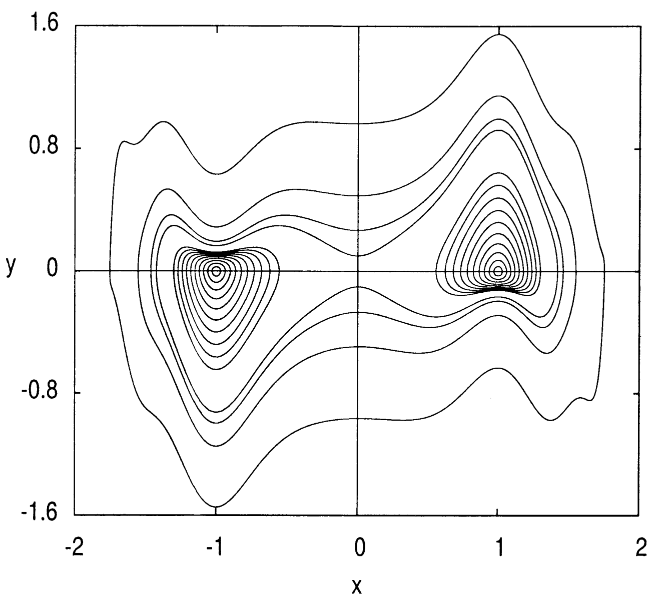

Fig. 16. The phase portrait of system (10) when $m = 10$, showing 19 limit cycles under the perturbed parameter values:

$$b = 1,$$

$$a_0 = -0.0095039920039995000099999600000299999990000000002,$$

$$a_1 = -0.768691720095992500079999880000000000001,$$

$$a_2 = -5.4005596080200049999000000199999997,$$

$$a_3 = 0.354894936223993000000000004,$$

$$a_4 = 15.1593602158920044999,$$

$$a_5 = -8.5477037360000005, \quad a_6 = -3.925792103996,$$

$$a_7 = 3.970000008, \quad a_8 = -0.841504,$$

$$a_9 = -0.0005, \quad a_{10} = 0.01.$$

5. Conclusion

In this paper, we have investigated limit cycles in a class of Liénard equation with $\deg(f) = 2m$ and $\deg(g) = 3$. Both local and global bifurcations are considered. The numbers of limit cycles are larger than expected, due to the symmetry of the system. A general proof needs to be developed to show that $\overline{H}(2m, 3) = 2m$ for any integer $m \geq 1$, and that the number of large limit cycles follows the rule given in Eq. (43).

Acknowledgment

This work was supported by the Natural Sciences and Engineering Research Council of Canada (NSERC).

References

Bautin, N. N. [1952] "On the number of limit cycles which appear with the variation of coefficients from an equilibrium position of focus or center type," *Mat. Sbornik* (*N.S.*) **30**, 181–196.

Han, M. [1999] "Liapunov constants and Hopf cyclicity of Liénard systems," *Ann. Diff. Eqs.* **15**, 113–126.

Han, M. [2002] *Periodic Solution and Bifurcation Theory of Dynamical Systems* (Science Publication, Beijing) (in Chinese).

Han, M., Lin, Y. & Yu, P. [2004] "A study on the existence of limit cycles of a planar system with

3rd-degree polynomials," *Int. J. Bifurcation and Chaos* **14**, 41–60.

Hilbert, D. [1902] "Mathematical problems," (M. Newton, Transl.) *Bull. Amer. Math.* **8**, 437–479.

Kukles, I. S. [1944] "Necessary and sufficient conditions for the existence of center," *Dokl. Akad. Nauk.* **42**, 160–163.

Li, J. & Liu, Z. [1991] "Bifurcation set and limit cycles forming compound eyes in a perturbed Hamiltonian system," *Publ. Math.* **35**, 487–506.

Li, J. [2003] "Hilbert's 16th problem and bifurcations of planar polynomial vector fields," *Int. J. Bifurcation and Chaos* **13**, 47–106.

Liénard, A. [1928] "Étude des oscillations entrenues," *Revue Génerale de l'Électricité* **23**, 946–954.

Liu, Y. & Li, J. [1989] "On the singularity values of complex autonomous differential systems," *Sci. in China* (*Series A*) **3**, 245–255 (in Chinese).

Lloyd, N. & Pearson, J. [2002] "Symmetry in planar dynamical systems," *J. Symb. Comput.* **33**, 357–366.

Lynch, S. [1999] "Generalized cubic Liénard equations," *Appl. Math. Lett.* **12**, 1–6.

Lynch, S. & Christopher, C. J. [1999] "Limit cycles in highly non-linear differential equations," *J. Sound Vibr.* **224**, 505–517.

Malkin, K. E. [1964] "Criteria for center of a differential equation," *Volg. Matem. Sbornik* **2**, 87–91.

Rayleigh, J. [1945] *The Theory of Sound* (Dover, NY).

Smale, S. [1998] "Mathematical problems for the next century," *The Math. Intell.* **20**, 7–15.

van der Pol, B. [1926] "On relaxation-oscillations," *Philos. Mag.* **7**, 901–912.

Yu, P. [1998] "Computation of normal forms via a perturbation technique," *J. Sound Vibr.* **211**, 19–38.

Yu, P. [2002] "Limit cycles in 3rd-order planar system," *Int. Congr. Mathematicians*, August 20–28, 2002, Beijing, China.

Yu, P. & Han, M. [2004] "Twelve limit cycles in a 3rd-order planar system with Z_2 symmetry," *Commun. Appl. Pure Anal.* **3**, 515–526.

Yu, P. & Han, M. [2005a] "Small limit cycles bifurcating from fine focus points in cubic order Z_2-equivariant vector fields," *Chaos Solit. Fract.* **24**, 329–348.

Yu, P. & Han, M. [2005b] "Twelve limit cycles in a cubic case of the 16th Hilbert problem," *Int. J. Bifurcation and Chaos* **15**, 2191–2205.

Zhang, T., Han, M., Zang, H. & Meng, X. [2004] "Bifurcation of limit cycles for a cubic Hamiltonian system under quartic perturbations," *Chaos Solit. Fract.* **22**, 1127–1138.